Taylor & Francis
Taylor & Francis Group

Polymer-Plastics Technology and Materials

ISSN: (Print) (Online) Journal homepage: www.tandfonline.com/journals/lpte21

Mechanical property characterizations of woven natural fiber-reinforced polymers 3D printed through a laminated object manufacturing process

Lai Jiang, Sazidur Shahriar, Md Shariful Islam, Tony Grady & Bryan Perez

To cite this article: Lai Jiang, Sazidur Shahriar, Md Shariful Islam, Tony Grady & Bryan Perez (02 May 2024): Mechanical property characterizations of woven natural fiber-reinforced polymers 3D printed through a laminated object manufacturing process, Polymer-Plastics Technology and Materials, DOI: 10.1080/25740881.2024.2347601

To link to this article: https://doi.org/10.1080/25740881.2024.2347601

Published online: 02 May 2024.

POLYMER-PLASTICS TECHNOLOGY AND MATERIALS
https://doi.org/10.1080/25740881.2024.2347601

Taylor & Francis
Taylor & Francis Group

Check for updates

Mechanical property characterizations of woven natural fiber-reinforced polymers 3D printed through a laminated object manufacturing process

Lai Jiang[a], Sazidur Shahriar[a], Md Shariful Islam[a], Tony Grady[b], and Bryan Perez[a]

[a]Department of Mechanical Engineering, Roy G. Perry College of Engineering, Prairie View A&M University, Prairie View, TX, USA; [b]Department of Chemistry, Brailsford College of Arts and Sciences, Prairie View A&M University, Prairie View, TX, USA

ABSTRACT
The mechanical properties of woven natural fiber reinforced polymers additively manufactured through Laminated Object Manufacturing (LOM) technology are investigated in this paper. The benefits of both the material and manufacturing process were combined into a sustainable practice, as a potential alternative to traditional synthetic composite materials made from non-renewable crude oil with limited end-of-life alternatives. Woven jute fiber reinforcements are used to strengthen both synthetic and bio- thermoplastic polymers in creating highly biodegradable composite structures. Such materials, as one of the prospective alternatives for synthetic composites, can be used in many engineering fields such as automobile panels, construction materials, and commodity and recreational products including sports and musical instruments. A LOM 3D printer prototype was designed and built by the authors. All woven jute/polymer biocomposite test specimens made using the built prototype in this study had their mechanical (both tensile and flexural) properties assessed using ASTM test standards and then compared to similar values measured from pure polymer specimens. Improved mechanical characteristics were identified and analyzed. Finally, SEM imaging was performed to identify the polymer infusion and fiber-matrix bonding conditions.

ARTICLE HISTORY
Received 31 December 2023
Revised 20 March 2024
Accepted 22 April 2024

KEYWORDS
Laminated object manufacturing (LOM); mechanical properties; PLA; polymers; prepregs; woven jute fiber

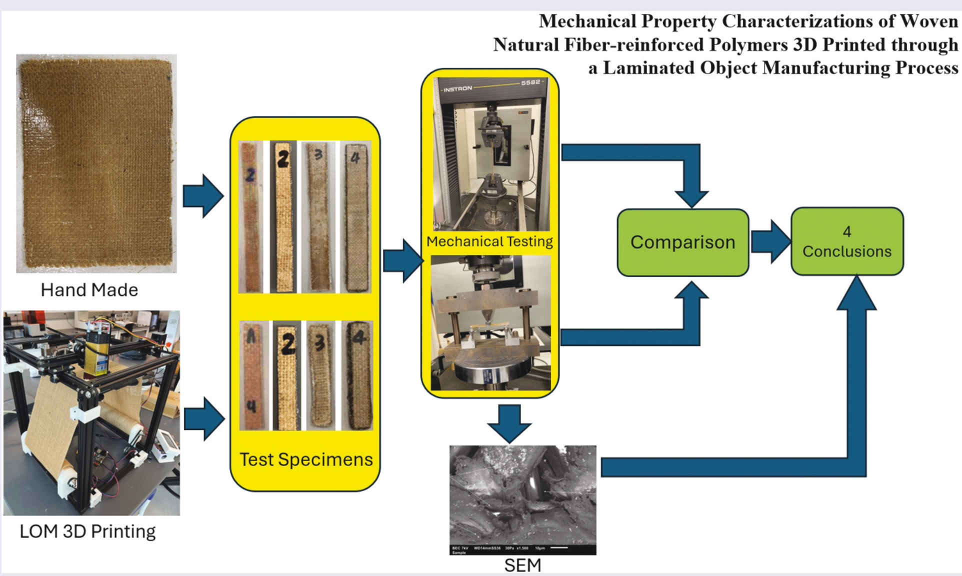

1. Introduction

The practice of creating three-dimensional engineering things directly from a 3D CAD or digital model is known as additive manufacturing. It is currently a large family of several different technologies that all function by adding layers of material to an existing item or substrate.[1] Laminated-object manufacturing (LOM) is one such technology that creates a solid physical model by stacking layers of sheet material that have each been cut to outlines that correspond to the cross-sectional forms of a CAD model that have been divided into layers.[2] To construct the part, cut layers are successively layered and bonded on

CONTACT Lai Jiang lajiang@pvamu.edu Department of Mechanical Engineering, Roy G. Perry College of Engineering, Prairie View A&M University, Prairie View, TX 77446, USA

top of the preceding ones. Excess material in each layer remains in situ to support the entire item during construction. Paper, cardboard, and plastic sheet stock with thicknesses ranging from 0.05 to 0.50 mm are common feedstock materials in LOM,[3] while many other engineering materials are being investigated and tested by researchers around the world: Klosterman et al.[4] created a curved layer LOM technique for monolithic ceramics (SiC) and ceramic matrix composites (SiC/SiC). The output of the process is a three-dimensional "green" ceramic that can be processed into a seamless, fully dense ceramic using conventional techniques. Windsheimer et al.[5] described the development and processing of a unique SiC-filler-loaded cellulosic paper (i.e., preceramic paper) using LOM with the ultimate goal of fabricating dense Si-SiC objects with complicated forms. In comparison to regular paper, preceramic paper contains a significantly higher level of the filler phase. These objects have pronounced anisotropy due to their laminar structure, which has a strong influence on their mechanical behavior. Yi et al.[6] studied the key LOM technologies for functional metal parts, employing sheet metal as the modeling material and diffusion welding technology to link cut sheet metal. Their sample part creation implies that the researched LOM technique with diffusion welding could be a valuable quick metal part manufacturing approach.

Other engineering materials being used for LOM include fiber-reinforced polymers. Pilipovic et al.[7] studied PVC parts made through LOM using a commercial SD 300 Pro LOM 3D printer. Tensile and flexural properties were measured using specimens 3D printed in different directions (x, y, and z). They found that polymer sheets are much better feedstock materials compared to paper for LOM as their mechanical properties are significantly improved and thus the application of such technology can be expanded. Kumar et al.[8] presented the LOM manufacturing of flexural test samples using ABS and thermoplastic polyurethane (TPU) polymers. The two polymer single layers were first FDM printed using two polymer filaments, and then LOM printed to form two types of sandwich specimens TPU-ABS-TPU (TAT)) and (ABS-TPU-ABS (ATA)). They found that ATA-based samples held greater flexural strength compared to TAT LOM samples, while the flexural strength of TAT composites significantly improved from about 6.8 MPa to 13 MPa (approximately 92% increase). Chang et al.[9] reported using continuous carbon fiber-reinforced thermoplastic composites (CF/PA6 prepregs) in a LOM 3D printing process, in which a laser beam was used in cutting the prepreg plies, and an ultrasonic roller was used for cut ply consolidation. 3D-printed composite parts were then measured for their tensile properties, with their unidirectional tensile strength reaching 1,760.2 MPa and elastic modulus of 105.7 GPa, both of which are superior in performance.

While synthetic fibers provide outstanding mechanical properties and allow for versatile design possibilities, environmental and economic considerations are driving research into the development and production of new materials for industries such as transportation, construction, and commodity and recreational products. New materials that are based on renewable natural resources and prevent further environmental stressors are of special importance.[10] Among these materials, natural fiber-reinforced polymers are gaining popularity as a potential replacement for glass fiber-reinforced polymer composites due to their numerous advantages such as low cost, biodegradability, low carbon footprint, acceptable mechanical properties, and society's emphasis on environmental issues and sustainability.[11–17] Biocomposite materials that combine natural fiber and biopolymers, which lead to fully biodegradable final products, are attracting much interest from many researchers.

Jute fibers were selected to be studied in this research as they can be obtained easily in fabric and fiber forms. They have a low density ($\rho = 1.3$ g/cm^3[11]) and good mechanical properties ($TS = 450$–550 MPa, $E = 26$–32 GPa[11]) compared to other natural fibers. Because of their high proportion of cellulose (61–72%), hemicellulose (14–20.4%), lignin (12–13%), and pectin (0.2%), these fibers are the most promising reinforcement materials extracted from the ribbon of the plant stem,[12] and has been used in many prior biocomposite materials manufacturing studies to reinforce other types of matrix.[13–18] In this paper, the prepreg sheet feedstocks for a custom-designed LOM 3D printing process were made using woven fabrics made from degummed jute fibers reinforcing both synthetic and bio- thermoplastic polymers. Mechanical properties of LOM 3D-printed biocomposite structures were measured, compared, and then analyzed.

2. Experimentation

2.1. The LOM 3D printer prototype

The authors designed and built a LOM 3D printer prototype (shown in Figure 1(a)), which can cut pre-made prepregs made from thermoplastic polymer-infused woven fibers with a 40W laser head. This prototype is equipped with an MKS DLC 32 motherboard and operated through an MKS TS35-R V2.0 touchscreen. The LOM system is programmed using G code. Five Tronxy SL42S TH40 stepper motors are used to control the X, Y,

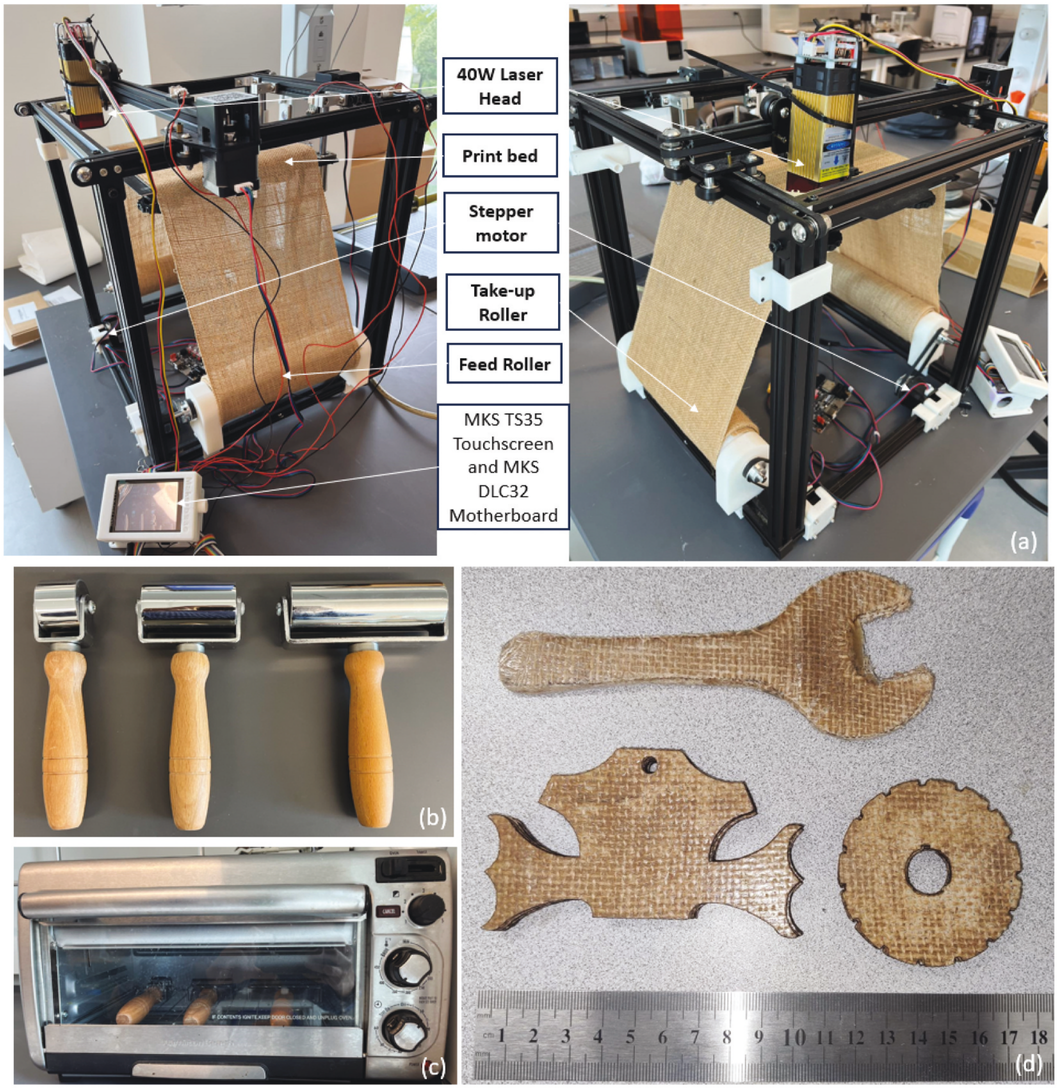

Figure 1. (a) The LOM 3D printer prototype designed and built by the research team, (b) metal rollers used to roll and press on the laser cut layer; (c) metal rollers being pre-heated to 200°C in an oven; (d) demo parts LOM printed by the LOM 3D printer.

and Z axes of the printing platform, and both the material feeding and the take-up rollers, respectively. The size of the printing platform is 220 × 220 × 300 mm. The pre-made prepreg is rolled onto both the material take-up rollers and feed rollers with its ends taped onto the roller surfaces. The tension of the prepregs is provided by both rollers that are connected to stepper motors via timing belts so the prepreg stays flat on the building platform. The material take-up roller pulls the prepreg roll forward while the feeding roller releases the same amount of prepregs when it's time to put a new layer of material onto the print platform. The laser head is controlled by the motherboard of the prototype through G-code for its movement, power, and on/off positions for cutting the prepreg. After the laser cuts the prepreg, a heated hand-held metal roller (shown in Figure 1(b) and (c)) is used to roll and press on the layer to partially melt the thermoplastic polymer so that the cut portions can be bonded onto the cut contours from the previous layer below. The material take-up roller then takes the unused materials away, leaving the laser-cut portions only in the building platform.

Figure 2. Woven jute textile used as reinforcements in this study.

This process allows the next layer of printing material to be placed just above the previous one, and the same process keeps repeating until all the layers of the model to be built are finished. The entire model is then removed from the LOM 3D printer prototype for post-processing. The printed parts will be placed onto a Carver 4120 thermal press to be thermally pressed at temperatures slightly above the melting temperature of the thermoplastic polymer for 15 min so the polymer can be remelted to have all layers better bonded together. Finally, parts are removed from the thermal press, cooled down, and manually trimmed to remove excessive polymers and fibers on the edges (shown in Figure 1(d)).

2.2. Materials

The natural fiber reinforcements used in this research are commercially available woven jute fabrics (shown in Figure 2) with a fiber density of 5 threads/cm and an average area density of 338 g/m^2. The average thickness is 0.071 mm for a single ply of this fabric.

Two types of thermoplastic polymers were used in this study:

(1) A commercial thermoplastic synthetic resin called Elium was developed by Arkema S.A.[19] The Elium 150 resin tested is a thermoplastic liquid polymer of low viscosity for reinforcement fiber infusion and resin transfer molding (RTM) processes. This resin allows the manufacturing of thermoplastic composites reinforced by continuous glass, carbon, or natural fibers using the same low-pressure techniques and equipment used to produce thermoset composite parts. Elium polymer with fiber reinforcement can be thermoformed under pressure and heat. This procedure necessitates heating the consolidated part for a few minutes at 180–200°C, followed by compression at a pressure ranging from 0.5 to 2 MPa, depending on the kind of reinforcement and composite part thickness.[20]

(2) Polylactic acid (PLA) biopolymer in the form of a white powder. PLA $(C_3H_4O_2)_n$[21] is a biopolymer that can be made at a reasonable cost nowadays using renewable resources. Because of the ester linkages that connect the monomer units, it is classed as an aliphatic polyester, which can degrade naturally in situ via a hydrolysis mechanism: Water molecules dissolve the ester bonds that make up the polymer backbone, resulting in a green matrix polymer substance.[22] When it comes to plastic filament for 3D printing, PLA is the most popular choice. Its low melting point, strong strength, little thermal expansion, good layer adhesion, and high heat resistance when annealed make it the perfect material for 3D printing applications such as biodegradable and biocompatible composite structures.[23] Without annealing, PLA is the least heat-resistant of the major 3D printing polymers.[23] The melting temperature of PLA is between 170°C and 180°C,[24] and the preferred forming pressure of jute/PLA biocomposites is 1.5 MPa [25].

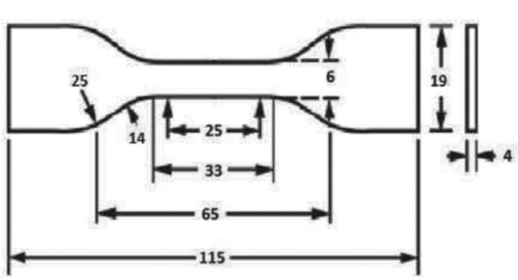

Figure 3. The dimension of dogbones made from pure polymers for tensile tests, all numbers in mm.

2.3. Mechanical test samples preparation

2.3.1. Pure polymer test specimens

For pure Elium test specimens, 3D CAD models with dimensions shown in Figure 3 for tensile tests and 73.2 mm × 12.7 mm × 3.0 mm for flexural tests, respectively, were created using SolidWorks, and then 3D printed using ABS plastic. These two 3D printed parts served as mold patterns. Blank rectangular blocks that are slightly larger than the desired specimen sizes were created using molding clay and the two 3D printed patterns were pressed into these blank blocks to make mold cavities. After all 10 clay molds were made, pure Elium thermoplastic resin was mixed with its hardener and then poured into pre-fabricated molds that were placed on the level lab bench and let cure for two days. The finished pure Elium polymer test specimens were obtained by removing the cured parts after destroying the clay molds.

For pure PLA test specimens, 3D CAD models were first created using SolidWorks software, and then FDM printed as solid (0% hollow inside) by a Raise3D Pro2 Plus 3D printer using pure PLA filaments. The dimensions of FDM printed pure PLA tensile and flexural test samples were 165 × 13 × 3.2 mm and 60 × 13.1 × 3.5 mm, respectively. All dimensions followed the values recommended by the ASTM D638–14 standard for tensile tests and the ASTM D790–10 standard for flexural tests.

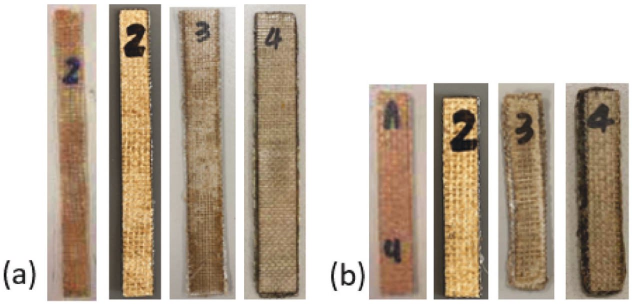

Figure 4. (a) Woven jute/polymer tensile test specimens from left to right: elium resin made through hand lay-up, elium resin made through LOM, PLA made through hand lay-up, and PLA made through LOM; (b) woven jute/polymer flexural test specimens from left to right: elium resin made through hand lay-up, elium resin made through LOM, PLA made through hand lay-up, and PLA made through LOM.

2.3.2. Jute/polymer test specimens made through hand lay-up

For making test specimens of jute/Elium polymer manually, continuous woven jute fabric was precut to sheets with a geometry of 127 × 254 mm. The Elium resin was applied onto both the top and bottom surfaces of a precut sheet by hand lay-up until both surfaces were fully covered and infused. The resin-infused layers were then stacked to reach the desired thickness and then sandwiched by two Dupont Kapton HN Films and thermally pressed for 10 min in the thermal press at 180°C under 0.5 MPa pressure to create biocomposite panels. In the case of abundant resin, some resin was squeezed out under pressure, indicating complete impregnation of the stacked plies. The Elium resin average weight ratio of the finished panels was measured to be 47.6%.

Similarly, PLA powders were evenly distributed onto cut woven jute fibers of the same size by hand lay-up and then stacked to reach the desired thickness, and then sandwiched by two Dupont Kapton HN Films, followed by thermal compressing at 180°C under 0.5 MPa pressure for 10–15 minutes to create biocomposite panels. The PLA polymer average weight ratio of the finished panels was measured to be 48.3%.

The panels were then used to cut for test specimens using a bandsaw. The dimensions of the tensile and flexural test specimens made from both prepregs were 139.7 × 12.7 × 1.5 mm and 73 × 12.7 × 3.43 mm, respectively (shown in Figure 4). All dimensions followed the values recommended by the ASTM D3039/D3039M–14 standard for tensile tests and the ASTM D7264/D7264M–07 standard for flexural tests.

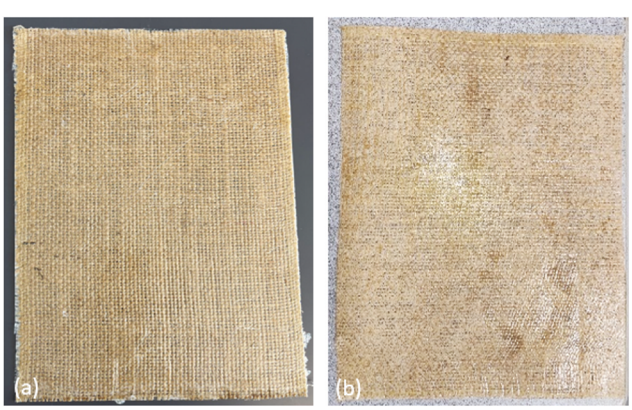

Figure 5. Pre-made (a) jute/Elium, (b) jute/PLA prepreg sections.

2.3.3. Jute/Polymer test specimens made through the LOM process

For making prepregs with the thermoplastic Elium resin, continuous woven jute fabric of 127 mm width was used. The liquid resin was applied onto both the top and bottom surfaces of a 127 × 524 mm area (due to the length of the thermal press platens) by hand lay-up until both surfaces were fully covered and infused. The resin-infused area was then sandwiched by two Dupont Kapton HN Films and thermally pressed for 10 min at 180°C under 0.5 MPa pressure. In the case of abundant resin, some resin was squeezed out under pressure, indicating complete impregnation of the fiber. This process was repeated until an entire roll of jute fabrics had been made into a prepreg roll. The Elium resin weight ratio of the finished prepreg was measured to be 48.8%. One section of the jute/Elium prepreg made is shown in Figure 5(a).

Similarly, PLA powders were evenly distributed onto woven jute fabrics of the same size by hand and then sandwiched by two Dupont Kapton HN Films, followed by thermal compressing at 180°C under 0.5 MPa pressure for 10–15 minutes. The PLA polymer weight ratio of the finished prepreg roll was measured to be 49.1%. One jute/PLA prepreg section made through this process is shown in Figure 5(b).

Prepregs made were then used by the LOM 3D printer prototype fabricated by the research team to make test specimens: laser-cut single-ply prepreg plies were stacked to reach the same test specimen thicknesses mentioned in Section 2.3.2 following ASTM D3039 and ASTM D7264 standards, and later moved to the thermal press for additional heated pressing at 180°C under 0.5 MPa pressure for 5 minutes to have all layers bond together. Tensile and flexural test samples of the same geometries were obtained (shown in Figure 4).

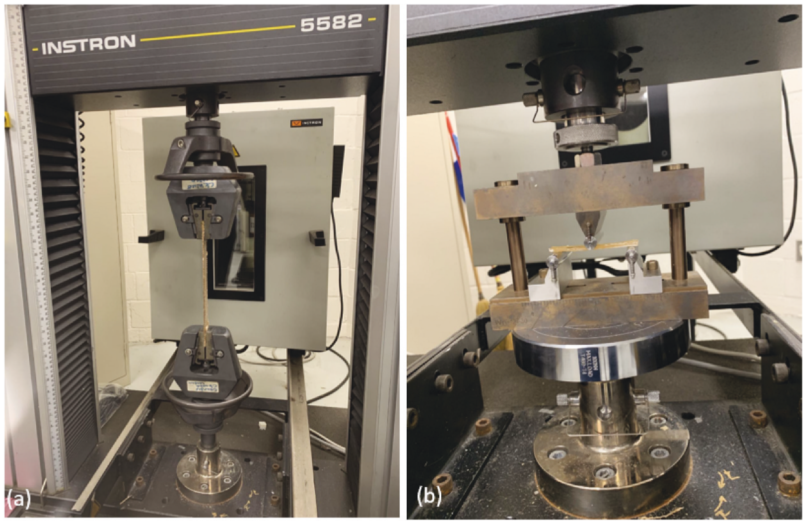

Figure 6. (a) Tensile testing fixture; (b) flexural testing fixture.

2.4. Test methods

2.4.1. Woven jute/polymer test specimen fiber volume fraction

ASTM D3171–22 Standard was followed in determining the fiber volume fractions of all woven jute/polymer test specimens made in Sections 2.3.2 and 2.3.3. The woven jute fabric's density was determined as below: First, a rectangular piece of cut jute woven fabric was weighted on a lab scale. Secondly, the average diameter of the yarns in the cut fabric was determined by measuring the diameters of different yarns at various locations and then calculating the average number. With this information, the average cross-sectional area of the yarns can be calculated. Thirdly, the number of yarns in both warp and weft directions were counted, with the length and width of the cut fabric, the volume of the cut jute fabric can be calculated. Finally, the density of the jute fabric can be calculated by dividing the fabric weight by the fabric volume. The thicknesses of all woven jute/polymer test specimens were measured using a digital caliper and the fiber volume fraction can be calculated using Eqution. 1:

$$V_r = \frac{0.1 A_r N_p}{\rho_r h} \tag{1}$$

2.4.2. Tensile test

An Instron 5582 Universal Testing Machine (UTM) was used for all tensile tests in this research (shown in Figure 6(a)). The fixture separations for all tensile tests used were 127.0 mm. Test speeds of the pure polymers and jute/polymer biocomposite were 5.0 mm/min (ASTM D638) and 2.0 mm/min (ASTM D3039), respectively. The tensile stress-strain data were automatically obtained by the UTM system. The ultimate tensile strengths were recorded with the maximum tensile stresses achieved in the tests, and elastic moduli were later obtained by calculating the average slope of tensile stress-strain curves of the five samples tested.

2.4.3. Flexural test

The same Instron UTM was used for all flexural tests (shown in Figure 6(b)), with the support spans of all flexural tests being 61.0 mm. Test speeds of both

Table 1. Measured thicknesses and fiber volume fractions of woven Jute/Polymer test specimens.

Material & Process	Average Thickness & Standard Deviation (mm)	Average Fiber Volume Fraction & Standard Deviation (%)
Jute/Elium Hand Tensile	1.428 ± 0.043	33.67 ± 0.99
Jute/Elium LOM Tensile	1.388 ± 0.033	34.63 ± 0.82
Jute/Elium Hand Flexual	3.425 ± 0.241	42.27 ± 3.21
Jute/Elium LOM Flexual	3.299 ± 0.065	38.85 ± 0.78
Jute/PLA Hand Tensile	1.408 ± 0.067	34.18 ± 1.58
Jute/PLA LOM Tensile	1.256 ± 0.026	38.27 ± 0.79
Jute/PLA Hand Flexual	3.363 ± 0.229	47.80 ± 3.38
Jute/PLA LOM Flexual	3.487 ± 0.210	50.67 ± 3.12

pure polymer samples and jute/polymer biocomposite structures were 1.0 mm/min (ASTM D790 and ASTM D7264, respectively). The flexural stress-strain data were automatically obtained by the UTM system. The ultimate flexural strengths were recorded with the maximum flexural stresses achieved in the tests, and flexural moduli were later calculated from the average slope of flexural stress-strain curves of the five samples tested.

2.4.4. SEM imaging

A JEOL JSM-6010LA Analytical Scanning Electron Microscope (SEM) was used for SEM imaging of failed biocomposite test specimens from tensile and flexural tests. The cross sections of biocomposite samples were obtained by cutting the failed specimens with a sharp utility knife and observed at 7kV under 30 Pa vacuum using different magnification levels. SEM images of typical locations at all observed cross-sections were obtained.

3. Results and discussion

3.1. Measured fiber volume fractions

The measured thicknesses and fiber volume fractions of all woven jute/polymer specimens are listed in Table 1. It can be seen that most of the specimens made had actual thicknesses that were slightly smaller than the target value (1.5 mm for tensile specimens and 3.43 mm for flexural specimens). This may be due to the pressure they carried during the thermal pressing processes. Additional layers are needed if a certain thickness is required for the biocompatible materials. Most jute/polymer biocomposite specimens had an average fiber volume fraction that is lower than 50%, which may cause insufficient mechanical properties of the finished biocomposite material.

3.2. Tensile properties

Measured tensile strengths and moduli of both pure polymers and woven jute/polymer biocomposites are

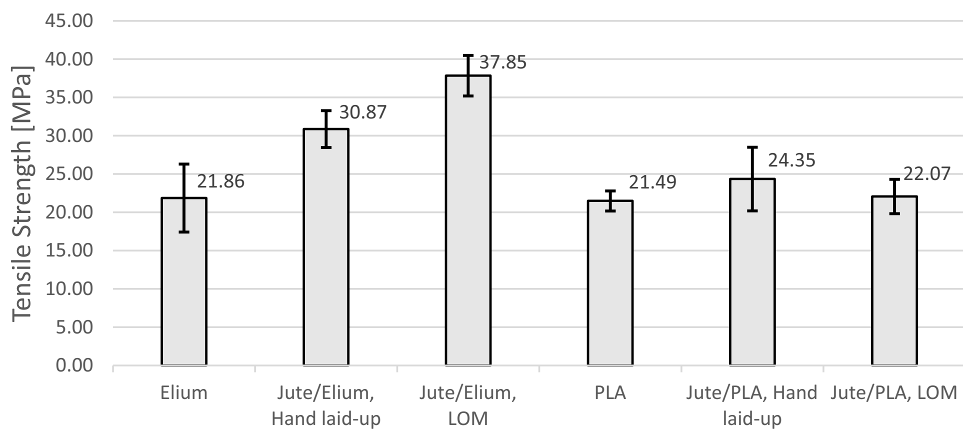

Figure 7. Tensile strengths comparisons of both polymers, their hand-laid-up, and LOM printed biocomposites.

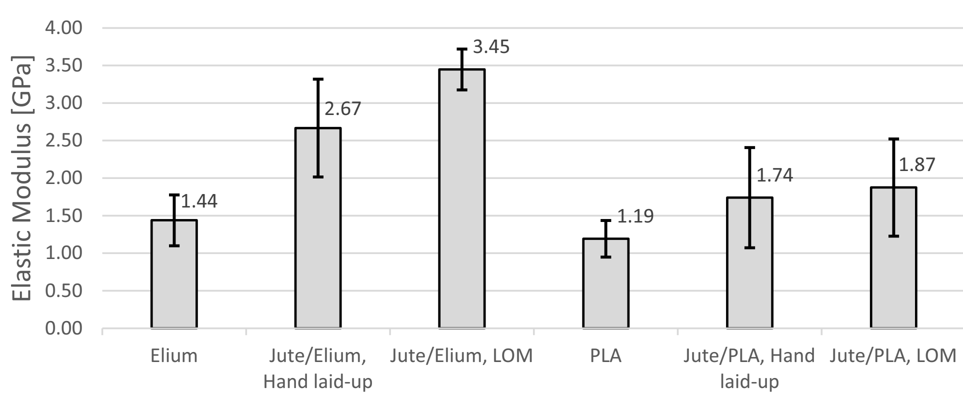

Figure 8. Elastic modulus comparisons of both polymers, their hand-laid-up, and LOM printed biocomposites.

shown in Figures 7 and 8, with standard deviation bars. It can be found that the cured pure Elium polymer has a higher tensile strength and elastic modulus compared to the FDM printed pure PLA biopolymer. The Elium polymer was significantly strengthened by the woven jute reinforcement fibers (41.2% increment in *TS* and 85.4% increment in *E* for the prepreg; 73.1% increment in *TS* and 83.3% increment in *E* for the LOM printed biocomposites). The PLA biopolymer was slightly strengthened by the woven jute reinforcement fibers in tensile strength (13.3% increment of the hand-laid-up and 2.7% increment of the LOM printed biocomposites) but was also greatly strengthened in elastic modulus (46.2% increment of the hand-laid-up and 57.1% increment of the LOM printed biocomposites). This may be caused by the pure PLA test specimens being FDM 3D printed using purchased PLA filament, while the jute/PLA hand-laid-up and LOM printed biocomposites were started from PLA powders. The solid powers may have difficulties in entering the gaps in the woven jute fibers to fill the voids therefore leaving relatively large amounts of voids in the finished biocomposite material. The tensile strength of the LOM printed jute/Elium biocomposite structure was further increased (22.6% increment) compared to the hand-laid-up ones, while the elastic modulus remained almost the same, this may be due to the second heating and pressing during the LOM process, leading to increased fiber volume fractions of the biocomposites and even stronger bondings between woven jute fiber and the Elium polymer. On the contrary, the measured tensile strength of the LOM printed jute/PLA biocomposite structure had a lower value than its hand-laid-up counterparts (9.4% reduction), while the elastic modulus was a little higher (7.5% increment). The low improvement of PLA matrix biocomposites may be due to the unevenly distributed dry PLA powders among woven jute fibers and layers, making it difficult to fill most of the gaps among the fiber and matrix, and therefore causing poor bonding situations between the fiber and PLA biopolymers. The highest tensile strength of woven jute/Elium biocomposites was determined to be 37.85 MPa, while the maximum elastic modulus was 2.67 GPa. The highest

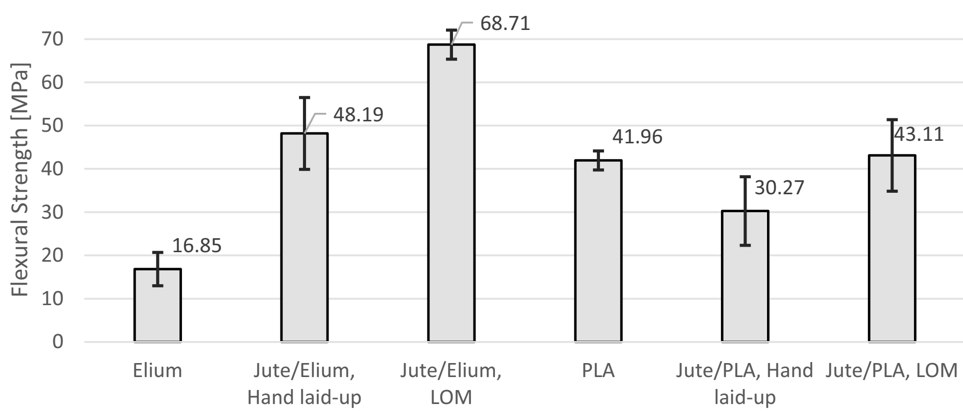

Figure 9. Flexural strengths comparisons of both polymers, their hand-laid-up, and LOM printed biocomposites.

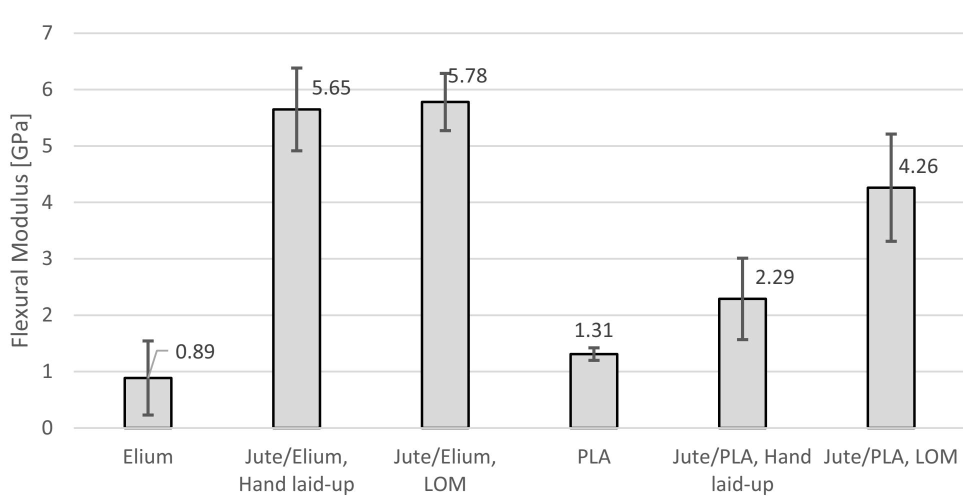

Figure 10. Flexural modulus comparisons of both polymers, their hand-laid-up, and LOM printed biocomposites.

tensile strength of woven jute/PLA biocomposites was measured to be 24.35 MPa, while the maximum elastic modulus was 1.87 GPa. LOM printed jute/PLA biocomposite structures are still weaker compared to the jute/Elium ones made.

3.3. Flexural properties

Measured flexural strengths and moduli of both polymers and woven jute/polymer biocomposites are displayed in Figures 9 and 10, with standard deviation bars. It can be found that the FDM printed PLA has a much higher flexural strength and modulus compared to the cured Elium polymer. The Elium polymer was significantly strengthened by the woven jute reinforcement fibers (96.4% difference in σ and 145.6% difference in E_f for the hand-laid-up biocomposites; 121.2% difference in σ and 146.6% difference in E_f for the LOM printed biocomposites). The PLA biopolymer was not quite strengthened by the woven jute reinforcement fibers in flexural strength (27.9% decrement of the hand-laid-up biocomposites but 2.7% increment of the

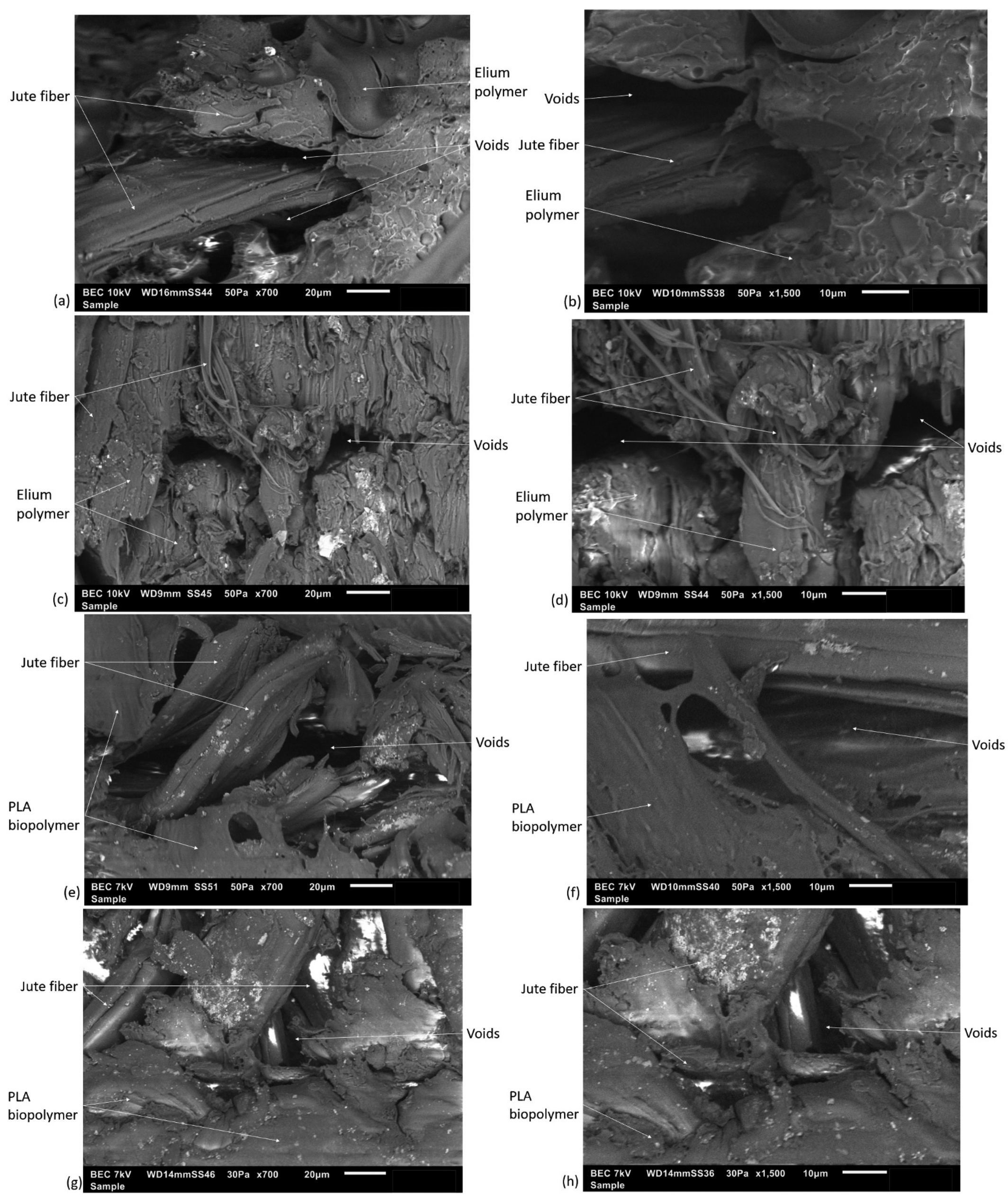

Figure 11. SEM imaging of biocomposites cross sections of (a, b) jute/Elium hand-laid-up biocomposites, (c, d) LOM printed jute/Elium biocomposites, (e, f) jute/PLA hand-laid-up biocomposites, (g, h) LOM printed jute/PLA biocomposites; (a, c, e, f are with a magnification of 700 ×, and b, d, e, g are with a magnification of 1,500 ×).

LOM printed biocomposites) but was again greatly strengthened in flexural modulus (74.8% increment of the hand-laid-up biocomposites and 106.0% difference of the LOM printed biocomposites). The high initial flexural strength of pure PLA is again due to the test specimens being FDM 3D printed using purchased PLA filament, while the jute/PLA prepregs and LOM printed biocomposites were started from PLA powders. The LOM process seems to further strengthen both jute/polymer biocomposites in both flexural properties. The highest flexural strength of woven jute/Elium biocomposites was determined to be 68.71 MPa, while the maximum elastic modulus was 6.85 GPa. The highest flexural strength of woven jute/PLA biocomposites was determined to be 43.11 MPa, while the maximum elastic modulus was 4.26 GPa. LOM printed jute/PLA biocomposite structures were weaker compared to the jute/Elium ones made. The major failing mechanism of jute/PLA test samples was debonding between adjacent layers due to interlaminar shear, which may be caused by the poor bonding properties at the fiber-matrix boundaries and among adjacent woven fiber plies of PLA.

3.4. SEM imaging

The SEM imaging results of the fiber-matrix boundaries of woven jute/polymer biocomposites are shown in Figure 11. It can be seen from Figure 11(a,b), the Elium polymer did not impregnate quite well into the jute fibers in the jute/Elium hand-laid-up biocomposites as there are very large void spaces. A similar situation can be seen in Figure 11(e,f) where the jute/PLA hand-laid-up biocomposites also have many voids inside the material. These voids prevent direct contact and binding between the reinforcement fiber and the polymer matrix and lead to poor mechanical properties of these two fiber-matrix combinations. It can be seen from Figure 11(c,d,g,h) that the void space inside the LOM 3D printed jute/Elium and jute/PLA structures has been reduced significantly compared to the 4 figures mentioned before, which indicates a better impregnation of the PLA polymer into the jute fiber. From Figure 11(c,g) at a magnification level of × 700, the polymer matrix is filled and binds better with the jute fibers than in Figure 11(a,b), while there are still some voids seen at some other locations in the biocomposites. At an even higher magnification level (×1,500) as shown in Figure 11(d,h), the same comparison can be performed with Figure 11(b,f). However, the LOM-printed jute/Elium biocomposite structure has higher measured mechanical properties compared to the LOM-printed jute/PLA biocomposite structure in the mechanical tests. This is due to the higher initial mechanical properties of the Elium polymer. Both LOM-printed biocomposite structures showed improved mechanical properties and fiber-matrix bondings compared to the hand-laid-up ones made using the same polymer, as shown in Figure 11(a–d and e–h), this is because the LOM-printed biocomposites were heated and pressed twice, allowing better distribution of both polymers in the structures and fiber-matrix bondings.

4. Conclusions

Based on the experimental validations reported above, the authors have proven that it is possible to 3D print laminated structures through the LOM process using woven natural fiber reinforced (bio)polymers. Such experimental validations have opened the door to further investigations of the LOM 3D printing technology applications in a sustainable manner using (bio)polymers reinforced by natural woven fibers in the future. From the measured mechanical properties of both types of pure polymers in this study, their woven jute fiber reinforced hand-laid-up biocomposites, and LOM printed biocomposite structures, the following conclusions can be made:

(1) The commercial Elium thermoplastic polymer has better measured tensile properties ($TS = 21.86$ MPa, $E = 1.44$ GPa) but weaker measured flexural properties ($\sigma = 16.85$ MPa, $E_f = 0.89$ GPa) compared to FDM-printed pure PLA. The addition of the woven jute fiber reinforcement significantly strengthened the Elium polymer in all four mechanical properties measured in this study, making its biocomposite structures strong in both tensile and flexural properties. This may be due to the good wet-through abilities of the liquid resin into the dry jute fiber when being applied to the biocomposites, which formed good bonding situations at the fiber-matrix interfaces.

(2) The FDM-printed pure PLA biopolymer has weaker measured tensile properties ($TS = 21.49$ MPa, $E = 1.19$ GPa) but better measured flexural properties ($\sigma = 41.96$ MPa, $E_f = 1.31$ GPa) compared to the commercial Elium thermoplastic polymer. Its combination with woven jute reinforcement fiber somewhat improved its mechanical properties but not as much as the case in the Elium polymer. This may be due to the already higher mechanical properties of the FDM-printed pure PLA material, and also the uneven distributions of the PLA powder when being

applied to dry jute fabrics which caused an incomplete impregnation during thermal pressing and therefore poor bonding between the reinforcement fiber and polymer matrix.

(3) The LOM printing process has positive impacts on the mechanical properties measured in this study. This is due to the same biocomposite material being heated up twice, allowing better distribution of polymers in the jute fiber and therefore improved fiber-matrix bondings. Excessive molten polymer was also squeezed out from the biocomposite structures and therefore their fiber volume fractions were increased. Major improvements can be found in both strengths and stiffnesses measured in this study. This finding has positive meanings for future studies and implementations in additive manufacturing using natural fiber reinforced polymers.

(4) The fiber-matrix bonding observed via SEM imaging shows gradual improvements in the fiber-matrix bondings of both jute/Elium and jute/PLA hand-laid-up biocomposites and LOM printed structures. Although the amount of voids at fiber-matrix interfaces is reduced and bonding improves, the overall fiber volume fractions of all made jute/polymer biocomposites made in this study are still not high enough (<50% in most cases). This is mainly due to the prepregging process as limited methods can be used to ensure the even and full impregnation of woven jute fibers, especially when using the solid PLA powder. Perhaps gradually increasing compressing pressure and platen temperature, and a longer compression molding time that slowly softens and melts the polymer and then forces it into the reinforcement fibers would provide better impregnation results. More research is still needed to further improve the fiber-matrix contacting areas and increase the fiber volume fractions of the biocomposite structures.

Acknowledgments

The National Science Foundation (NSF) of the United States supported this research with grant #1909699.

Disclosure statement

No potential conflict of interest was reported by the author(s).

Funding

The work was supported by the National Science Foundation [#1909699].

Notes on contributors

Lai Jiang Associate professor of Mechanical Engineering at Prairie View A&M University. His research area includes (bio)composite materials and manufacturing, manufacturing process simulations, machine and tooling design and fabrication, etc.

Sazidur Shahriar Master of Science in Mechanical Engineering at Prairie View A&M University.

Md Shariful Islam Master's student in Mechanical Engineering at Prairie View A&M University.

Tony Grady Technician of Analytical Chemistry at the Department of Chemistry at Prairie View A&M University.

Bryan Perez Undergraduate student in Mechanical Engineering at Prairie View A&M University.

References

[1] Ngo, T. D.; Kashani, A.; Imbalzano, G.; Nguyen, K. T.; Hui, D. Additive Manufacturing (3D Printing): A Review of Materials, Methods, Applications and Challenges. *Compos. B Eng.* 2018, *143*(15), 172–196.

[2] Jarosinski, W.; Zhang, J. Additive Manufacturing Processes and Equipment. In *Additive Manufacturing - Materials, Processes, Quantifications and Applications*; Jing, Z., Yeon-Gil J., Eds.; Oxford, UK: Butterworth-Heinemann, 2018; pp. 39–51.

[3] Groover, M. Rapid Prototyping and Additive Manufacturing. In *Fundamentals of Modern Manufacturing - Materials, Processes, and Systems*; Mikell P. G., Eds.; John Wiley & Sons: Danvers, MA, 2016; pp. 716–733.

[4] Klosterman, D.; Chartoff, R.; Osborne, N.; Graves, G.; Lightman, A.; Han, G.; Bezeredi, A.; Rodrigues, S. Development of a Curved Layer LOM Process for Monolithic Ceramics and Ceramic Matrix Composites. *Rapid. Prototyping. J.* 1999, *5*(2), 61–71. DOI: 10.1108/13552549910267362.

[5] Windsheimer, H.; Travitzky, N.; Hofenauer, A.; Greil, P. Laminated Object Manufacturing of Preceramic-Paper-Derived Si-SiC Composites. *Adv. Mat.* 2007, *19*(24), 4515–4519. DOI: 10.1002/adma.200700789.

[6] Yi, S.; Liu, F.; Zhang, J.; Xiong, S. Study of the Key Technologies of LOM for Functional Metal Parts. *J. Mater. Process. Technol.* 2004, *150*(1–2), 175–181. DOI: 10.1016/j.jmatprotec.2004.01.035.

[7] Pilipovic, A.; Raos, P.; Sercer, M. Experimental Testing of Quality of Polymer Parts Produced by Laminated Object Manufacturing - LOM. *Tech. Gaz.* 2011, *18*(2), 253–260.

[8] Kumar, S.; Singh, I.; Koloor, S. S.; Kumar, D.; Yahya, M. Y. On Laminated Object Manufactured FDM-Printed ABS/TPU Multimaterial Specimens: An Insight into Mechanical and Morphological Characteristics. *Polymers*. 2022, *14*(4066), 14194066. DOI: 10.3390/polym14194066.

[9] Chang, B.; Parandoush, P.; Li, X.; Ruan, S.; Shen, C.; Behnagh, R. A.; Liu, Y.; Lin, D. Ultrafast Printing of

Continuous Fiber-Reinforced Thermoplastic Composites with Ultrahigh Mechanical Performance by Ultrasonic-Assisted Laminated Object Manufacturing. *Polymer. Compos*. 2020, *41*(11), 4706–4715. DOI: 10.1002/pc.25744.

[10] Pozzi, A.; Sepe, R., "Mechanical Properties of Woven Natural Fiber Reinforced Composites," in *ECCM15 15th European Conference on Composite Materials*, Venice, 2012.

[11] Salman, S. D. Effects of Jute Fibre Content on the Mechanical and Dynamic Mechanical Properties of the Composites in Structural Applications. *Defence. Technol*. 2020, *16*(6), 1098–1105. DOI: 10.1016/j.dt.2019.11.013.

[12] Dalbehera, S.; Acharya, S. Study on Mechanical Properties of Natural Fiber Reinforced Woven Jute-Glass Hybrid Epoxy Composites. *Adv. Polymer. Sci. Tech*. 2014, *4*(1), 1–6.

[13] Jiang, L.; Peng, X.; Walczyk, D. F. 3D Printing of Biofiber-Reinforced Composites: A Review. *Rapid Prototyp. J*. 2020, *26*(6), 1113–1129. DOI: 10.1108/RPJ-08-2019-0214.

[14] Jiang, L.; Walczyk, D.; Li, B. Modeling of Glue Penetration into Natural Fiber Reinforcements by Roller Infusion. *J. Manuf. Sci. Eng*. 2018, *140*(4), 041006–1–11. DOI: 10.1115/1.4038514.

[15] Jiang, L.; Walczyk, D.; McIntyre, G. A New Approach to Manufacturing Biocomposite Sandwich Structures: Investigation of Preform Shell Behavior. *J. Manuf. Sci. Eng*. 2017, *139*(2), 021014–1–11. DOI: 10.1115/1.4034278.

[16] Jiang, L.; Walczyk, D.; McIntyre, G.; Bucinell, R.; Li, B. Bioresin Infused Then Cured Mycelium-Based Sandwich-Structure Biocomposites: Resin Transfer Molding (RTM) Process, Flexural Properties, and Simulation. *J. Cleaner Prod*. 2019, *207*, 123–135.

[17] Jiang, L.; Walczyk, D.; McIntyre, G.; Chan, W. K. Cost Modeling and Optimization of a Manufacturing System for Mycelium-Based Biocomposite Parts. *J. Manufactur. Syst*. 2016, *41*, 8–20. DOI: 10.1016/j.jmsy.2016.07.004.

[18] Jiang, L.; Walczyk, D.; McIntyre, G.; Bucinell, R.; Tudryn, G. Manufacturing of Biocomposite Sandwich Structures Using Mycelium-Bound Cores and Preforms. *J. Manuf. Processes*. 2017, *28*, 50–59. DOI: 10.1016/j.jmapro.2017.04.029.

[19] Arkema. brochure-elium-2017. Arkema, [Online]. 2017. Available: https://www.arkema.co.jp/export/shared/.content/media/downloads/products-documentations/incubator/brochure-elium-2017.pdf. [Accessed Jun 25, 2023].

[20] Arkema. Elium 150 Technical datasheet. Arkema, [Online]. Available: https://cstjmateriauxcomposites.files.wordpress.com/2017/11/elium_150_tech_data_sheet_grp_160908.pdf. [Accessed Jun 25, 2023].

[21] Jiang, X.; Luo, Y.; Tian, X.; Huang, D.; Reddy, N.; Yang, Y. Chemical Structure of Poly(Lactic Acid). In *Poly(Lactic Acid): Synthesis, Structures, Properties, Processing, and Applications*; Rafael A., Loong-Tak L., Susan E. M. S., Hideto T., Eds.; Hoboken, New Jersey, US: John Wiley and Sons, 2010; pp. 69–82.

[22] Casalini, T.; Rossi, F.; Castrovinci, A.; Perale, G. A Perspective on Polylactic Acid-Based Polymers Use for Nanoparticles Synthesis and Applications. *Front. Bioeng. Biotechnol*. 2019, *7*, 259. DOI: 10.3389/fbioe.2019.00259.

[23] Nagarajan, V.; Mohanty, A. K.; Misra, M. Perspective on Polylactic Acid (PLA) Based Sustainable Materials for Durable Applications: Focus on Toughness and Heat Resistance. *ACS Sustain. Chem. Eng*. 2016, *4*(6), 2899–2916.

[24] Kaczmare, H.; Nowicki, M.; Vuković-Kwiatkowska, I. Crosslinked Blends of Poly(lactic Acid) and Polyacrylates: AFM, DSC and XRD Studies. *J. Polym. Res*. 2013, *20*(3), 91.